Drug Design

Binding Mode Determination of Benzimidazole Inhibitors of the Hepatitis C Virus RNA Polymerase by a Structure and Dynamics Strategy**

Steven R. LaPlante, Araz Jakalian, Norman Aubry, Yves Bousquet, Jean-Marie Ferland, James Gillard, Sylvain Lefebvre, Martin Poirier, Youla S. Tsantrizos, George Kukolj, and Pierre L. Beaulieu*

Infection by the hepatitis C virus (HCV) is a serious cause of chronic liver disease worldwide, with more than 170 million infected individuals at significant risk of mortality.[1] Though an immunomodulator treatment of limited efficacy exists, there is an urgent need for potent drugs which can specifically target the viral proteins.[2] The HCV-encoded NS5B RNA-

[*] Dr. S. R. LaPlante, A. Jakalian, N. Aubry, Y. Bousquet, J.-M. Ferland, J. Gillard, S. Lefebvre, M. Poirier, Y. S. Tsantrizos, G. Kukolj, P. L. Beaulieu
Departments of Chemistry and Biological Sciences
Boehringer Ingelheim (Canada) Ltd., Research and Development
2100 Cunard St., Laval, Quebec (Canada) H7S2G5
Fax: (+1) 450-682-8434
E-mail: slaplante@lav.boehringer-ingelheim.com

[**] We are grateful to Dr. Michael Bös, Dr. Michael Cordingley, and Dr. Paul Anderson for encouragement and support. We also thank Dr. Timothy Stammers, Dr. Nathalie Goudreau, Dr. Marc-André Poupart, Dr. Dale Cameron, and Mr. Jeff O'Meara for comments or critical reading of the manuscript, as well as Ginette McKercher for determining inhibition constants.

Supporting information for this article is available on the WWW under http://www.angewandte.org or from the author.

  DOI: 10.1002/ange.200460326

dependent RNA polymerase is essential for viral replication and has long been considered an attractive target for therapeutic intervention in HCV-infected patients.[3]

Herein, we report the application of structure- and dynamics-based strategies for determining the binding mode of novel benzimidazole inhibitors of the HCV polymerase. We demonstrate that a screen-derived compound binds directly to NS5B, and determine the polymerase-bound structure of a potent analogand upon binding the polymerase, and elucidate the principle binding roles of each of the substituents. Besides providing medicinal chemists with practical information for designing HCV polymerase inhibitors, the methodology has general utility and can be applied to most ligand–macromolecule systems for studying molecular recognition processes.

Our search for potential leads for inhibitors of NS5B polymerase (HCV polymerase) began by using a high-throughput screen (HTS) of our compound collection, from which compound **1** was identified.[4] In addition to our

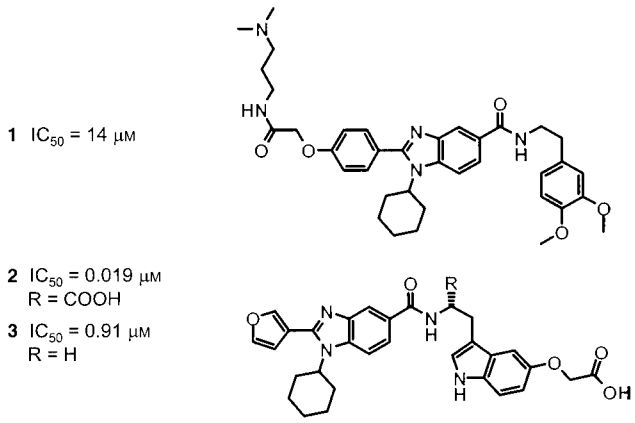

biochemical specificity assays,[4] differential line broadening (DLB) NMR experiments[5,6] played an important role in demonstrating that **1** binds directly to HCV polymerase and not to RNA, a substrate in the HTS screen and specificity assays. Figure 1a shows that a ^{1}H NMR resonance of free **1** (blue) incrementally broadened upon addition of HCV polymerase (red), whereas broadening was not detected in the presence of RNA (blue versus red, Figure 1b). The observed broadening is a result of fast-exchange binding (on the NMR timescale) to the polymerase and is an average of the linewidths and chemical shifts of the free and bound states. A higher stoichiometry of ligand was employed to simplify signal detection. Having identified compound **1** as a valid lead compound,[4,7] we subsequently synthesized numerous analogues and discovered potent compounds such as **2**,[7,8] which has a truncated left side and a more optimal right side that imparts a 738-fold improvement in potency. The discovery process for these compounds[4,7,8] involved the development of structure–activity relationships (SAR), assistance from combinatorial chemistry, and the elucidation of the binding role of each substituent.

As part of our inhibitor-optimization effort, several NMR spectroscopic methods were used to monitor direct binding to HCV polymerase. ^{1}H DLB experiments provided a straightforward and practical tool. Notably, specific resonances in the ^{1}H spectrum of free compound **2** and the related analogue **5** (blue spectra in Figure 1d,e, respectively) differentially broadened in the presence of relatively small amounts of HCV polymerase (red). ^{19}F NMR experiments also provided evidence of direct binding. The sharp trifluoromethyl resonance of free compound **4** (blue spectrum in Figure 1c) broadened and shifted upon binding to the HCV polymerase (red spectra). Unlike the ^{1}H DLB experiment which employed an excess of inhibitor, the ^{19}F NMR data were acquired at a 1:1 inhibitor:polymerase ratio and thus provided the additional advantage of potentially monitoring the number of binding sites. The observation of a single, bound ^{19}F resonance in Figure 1c (red) is consistent with a single binding site. Finally, a ^{1}H transferred NOESY experiment[5,6] was also applied to detect the binding of **1** (see Supporting Information) and **2**. The NOESY spectrum of free **2** (Figure 2a) lacks crosspeaks, as would be expected for a fast-tumbling small molecule. In the presence of HCV polymerase, multiple negative-sign crosspeaks appear as a result of fast-exchange binding to the slower tumbling HCV polymerase (Figure 2b).

The "transferred" NOESY crosspeaks in Figure 2b also reflect a fingerprint of short, intramolecular hydrogen bonds when compound **2** is bound to the polymerase. Overall, the ensemble of data was suggestive of a single, bound conformation with the exception of two potential orientations of the benzoic acid–amide bond. On the basis of the transferred NOESY crosspeaks, distance-restrained simulated-annealing calculations were applied to determine the bound structure of **2**. Two possible 3D structures, that differed only in the orientation of the benzoic acid–amide bond, were determined by calculations that varied only by the inclusion of an H15 to H4 restraint (herein defined as the "NH up" orientation, Figure 2c), or the inclusion of an H15 to H6 restraint (herein defined as the "NH down" orientation, Figure 2d). A definition of the atom numbering scheme is provided in Figure 1e.) Although both corresponding NOESY crosspeaks of equal intensity were observed and suggested a perpendicular amide–benzimidazole orientation, our ab initio calculations were more consistent with the existence of either or both energetically favorable coplanar orientations (see the Supporting Information). It is also possible and likely that one of the NOESY crosspeaks was an artifact of spin-diffusion contamination[6] and experimental attempts to resolve the problem were unsuccessful (that is, very short mixing times, QUIET-NOESY, etc.). Hence, we resorted to the design of azabenzimidazole **7** as a conformational probe in which the carbon atom at position Y was substituted by a nitrogen atom. This compound was predicted by ab initio calculations to preferentially adopt the coplanar NH up orientation of the benzoic acid–amide bond in the free state as a result of a favorable electrostatic interaction between the NH and lone-pair of electrons on the nitrogen atom. This preferential orientation in the free state was also observed by ROESY NMR experiments (see the Supporting Information), and is consistent with the bound structure in Figure 2c since compounds **6** (Y = CH) and **7** (Y = N) exhibit similar affinity

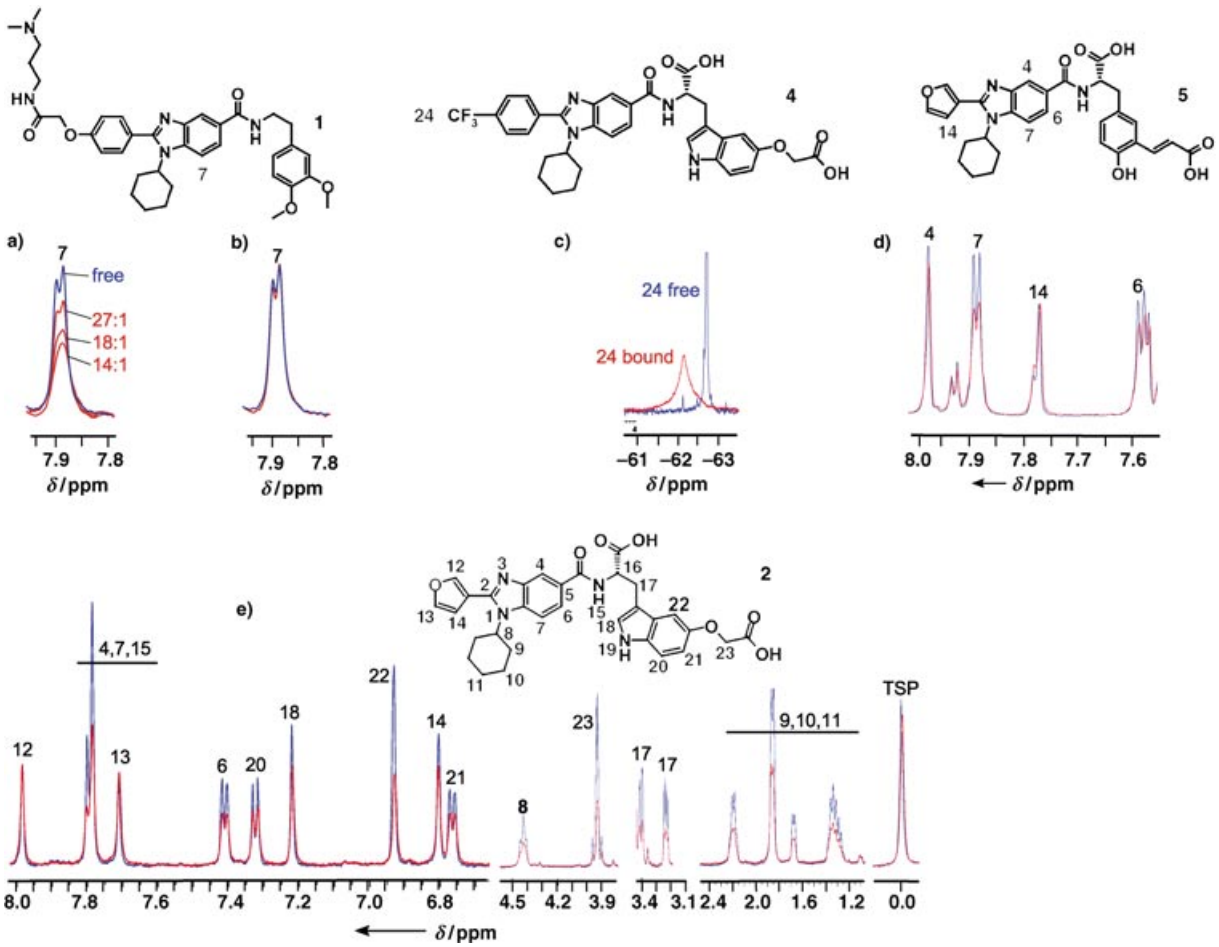

Figure 1. ^{1}H DLB and ^{19}F NMR resonance broadening for monitoring the binding to HCV polymerase. a) The ^{1}H resonance of H 7 of **1** in the absence (blue) and in the presence (red) of incremental amounts of HCV polymerase (at inhibitor to polymerase ratios of 27:0, 18:1, and 14:1). The NS5BΔ21C-HT polymerase construct was used for all NMR studies. b) The ^{1}H resonance of H 7 of **1** in the absence (blue) and in the presence (red) of tRNA (at an inhibitor to tRNA ratio of 14:1). c) ^{19}F NMR spectra (scaled as ppm) in the absence (blue) and in the presence (red) of HCV polymerase at an inhibitor to polymerase ratio of 1:1. An IC_{50} value of 0.5 μM was measured for compound **4**. d) A subregion of the ^{1}H spectra (scaled in ppm) of **5** in the absence (blue) and in the presence (red) of HCV polymerase at an inhibitor to polymerase ratio of 70:1. The hydrogen assignments are provided above each resonance. An IC_{50} value of 0.03 μM was measured for compound **5**. e) Subregions of the ^{1}H spectra (scaled in ppm) of **2** in the absence (blue) and in the presence (red) of HCV polymerase at an inhibitor to polymerase ratio of 70:1. The hydrogen assignments are provided above each resonance. The resonances of the spectator molecule [2,2,3,3-D_4]3-trimethylproprionic acid (TSP) were used to normalize the resonance intensities.

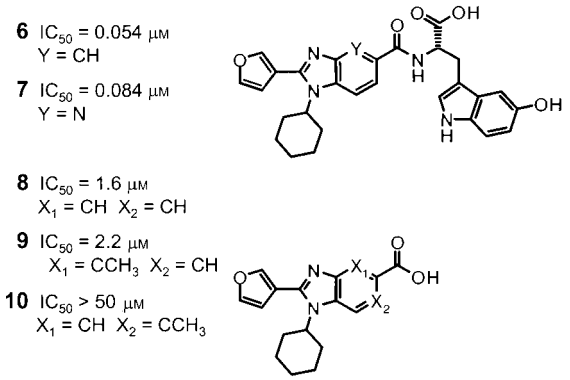

for the polymerase. In conclusion, the 3D bound structure in Figure 2c provided the first insight into the bioactive conformation of this class of compounds. Notably, the cyclohexyl and furan planes are perpendicular with respect to the benzimidazole scaffold, and the tryptophan residue on the right side extends above and perpendicular to the benzimidazole plane giving the molecule an overall L shape.

We also investigated the binding roles of the individual substituents of this class of compounds to support medicinal and combinatorial chemistry efforts. First, the importance of the cyclohexyl group became evident given that replacement with a hydrogen atom resulted in a greater than 116-fold loss in potency, and only very conservative replacements of the cyclohexyl group were tolerated.[7] We also observed significant DLB for the NMR resonances of the cyclohexyl ring (H8–H11) of compound **2** in the presence of the polymerase (red spectrum, Figure 1e). Thus, the data taken together is consistent with the cyclohexyl group having a direct role in binding, and it highlights the application of DLB as a tool for epitope mapping, as we reported elsewhere.[5]

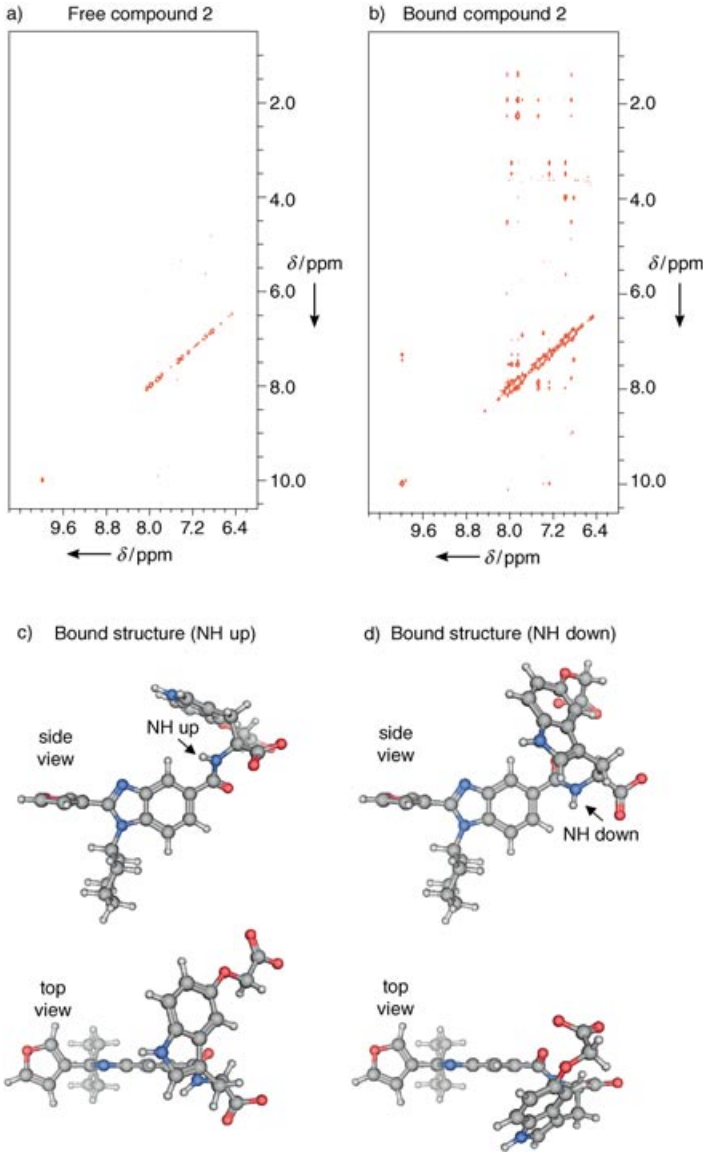

Figure 2. Monitoring of the binding and determination of the bound structures of compound **2**. a) The amide/aromatic (horizontal axis) to aliphatic (vertical axis) subregion of the ^{1}H NOESY spectrum of free compound **2** (75 msec mixing time). b) A subsequent NOESY experiment is shown after the addition of polymerase (NS5BΔ21-His$_6$ construct) to the NMR sample tube (transferred NOESY data were acquired at a 70:1 inhibitor to polymerase ratio). c) A representative structure of **2** when bound to HCV polymerase as determined by a simulated annealing calculation that employed restraints derived from transferred NOESY data. The calculations included a restraint between H15 and H4 (and none between H15 and H6, see the numbering scheme for the hydrogen atoms in Figure 1e). d) Another possible structure of **2** when bound to HCV polymerase for which the calculations included a restraint between H15 with H6 (and none between H15 with H4). The structures in (c) and (d) are colored by atom-type (oxygen: red, nitrogen: blue, carbon: gray, hydrogen: white). It must be kept in mind that determination of the 3D structures is limited by the inherent pseudosymmetry of the compound. Given the C_2 pseudosymmetry along the benzimidazole plane, the furan ring can adopt the bound conformations shown in (c) (top view) and/or an orientation rotated by approximately 180° along the carbon C_2-furan axis (see Figure 1e for a definition of the atom numbering scheme employed).

Elucidation of the principle role of the C2 substituent was also pursued. Initially, we observed the lack of DLB for the ^{1}H NMR resonances of the extended left side of compound **1**.[7] This observation suggested that these hydrogen atoms experienced insignificant changes in their magnetic environments upon binding, as one would expect if they were exposed to solvent in both the free and bound states. It was also consistent with our finding that partial truncation of the left side resulted in no significant change in the binding affinity for the polymerase.[7] Similarly, the lack of DLB observed for H12–H14 of the furan ring at position 2 of compound **2** (Figure 1e) also suggested that it experiences a minimal, direct contact with the polymerase, and it is consistent with our results obtained from studies of structure–activity relationships[7] which showed that the furan ring can be substituted by a variety of aromatic groups with little effect on potency. However, replacement of the furan ring by a hydrogen atom resulted in a 30-fold loss in potency.[7] One possible explanation is that the furan ring doesn't directly contact the polymerase, but instead influences the conformation of the critical cyclohexyl ring in the free state. We applied ab initio calculations to monitor the preferred orientations of the S_1 torsion angle (defined by the C8–N1 bond in Figure 3c) of compound **2** versus that of a model compound in which the furan ring is replaced by a hydrogen atom. The calculations determined that a single, lowest-energy torsion angle at approximately 0° was preferred for compound **2**, with high-energy barriers to rotation (Figure 3a). In contrast, the calculations involving the model compound (Figure 3b) exhibited two lowest-energy torsion angles at about 180 and 0° with much lower energy barriers to rotation. Thus, the furan ring apparently contributed to orienting the cyclohexyl ring of the free compound (ca. 0° for S_1) to a conformation that resembled the bound state (ca. 0° for S_1 in Figure 2c and d). As further validation, ROESY data on the free state of compound **2** and transferred NOESY data on the bound state exhibit similar crosspeak patterns that are indicative of a preference for a 0° torsion angle along S_1. Spectra in the Supporting Information show large crosspeaks between H8 with H14 and H12, as well as smaller crosspeaks between H8 and H7. Furthermore, a restricted rotation about the C8–N1 bond was also consistent with the relatively short ^{13}C spin-lattice relaxation times (^{13}C T_1) for the C8 and C11 atoms of the cyclohexyl ring of compound **2** (Figure 3c, numbers in round brackets). ^{13}C T_1 values are sensitive to motions on the pico- to nanosecond time scale and represent an excellent NMR parameter for monitoring the relative flexibility of C-H vectors. Shorter times are indicative of relatively slower segmental motion or flexibility. In summary, the conformational restriction induced by the furan ring results in a minimization of the overall entropic cost of binding.

The function of the benzimidazole ring was also investigated. Its role as a scaffold that orients the three appendages in 3D space is visible in Figure 2c and d. In addition, our DLB data also showed significant DLB for H6, which suggests that this portion of the ring contacts the

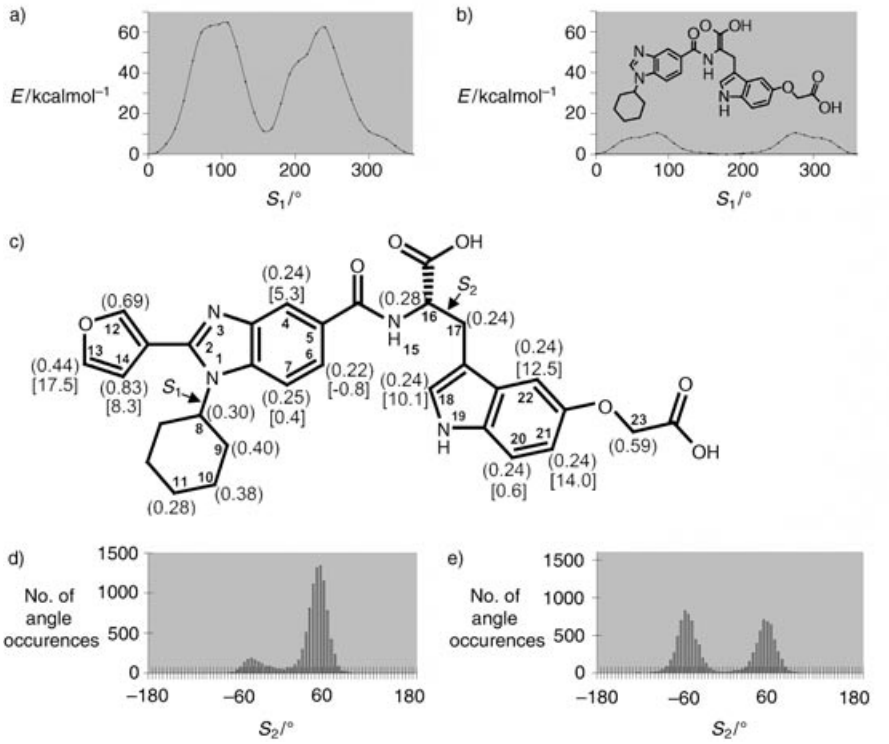

Figure 3. Monitoring the flexibility (dynamics) attributes of free and bound compound **2** and free compound **3**. a) ab initio RHF/6-31G** calculations of compound **2** in which the energy is determined for each torsion angle value of S_1 along the N1–C8 bond. The torsion angle is defined as the C2-N1-C8-H8 atoms. The atom numbering scheme is shown by the numbers with no brackets. b) Similar calculations are reported for a model compound that is similar to **2** with the exception that the furan ring is replaced by a hydrogen atom. c) ^{13}C NMR T_1 relaxation times (seconds) are displayed (round brackets) beside each carbon atom for compound **2** (data are derived from the compound in [D$_6$]DMSO). In the cases where two hydrogen atoms are attached to a single carbon atom, NT_1 data are given (the product of the number of attached protons and the longitudinal relaxation time). Transferred ^{13}C T_1 relaxation data are displayed within square brackets. The values displayed are the percentage change from free versus that after addition of the polymerase (NS5BΔ21-HT construct). Data were acquired using aqueous buffer (see Supporting Information). Transferred ^{13}C T_1 data were not acquired for the aliphatic carbon atoms. d) Histogram of torsion angle S_2 of compound **2** sampled during a 1 nsec molecular dynamics simulation. The S_2 torsion angle is defined by the indole atoms C-C17-C16-H16, see (c). e) A similar histogram as in (d) is shown except that compound **3** was studied.

polymerase (Figure 1e). The resonances of H4 and H7 were superimposed with H15 (Figure 1e), which unfortunately hindered interpretation. However, observations were possible for these hydrogen atoms in the closely related analogue **5** (Figure 1d), in which the resonances of H7 and H6 were line-broadened and H4 was relatively less affected, thus suggesting that the former were exposed to the polymerase pocket whereas the latter was exposed to the solvent in the bound state. These observations were further probed by monitoring changes in the binding affinity upon addition of bulky methyl groups at the C4 or the C6 positions in a related, truncated series (that is, **8**–**10**). It was noteworthy that **9** ($IC_{50} = 2.2$ μM), which is methylated at position C4 (defined as X_1), had similar potency relative to the unmethylated analogue (**8**, $IC_{50} = 1.6$ μM), thus suggesting that the methyl group was likely exposed to the solvent. In contrast, methylation at the C6 position (defined as X_2) resulted in a >31-fold loss in potency (**10**, $IC_{50} > 50$ μM), which suggests that it unfavorably bumped into the polymerase surface. Thus, it appeared that the lower part of the benzimidazole participated in direct binding to the polymerase pocket, whereas the upper part was exposed to the solvent.

Our studies also probed the binding role of the carboxylic acid at position C16 of compound **2**. Its importance was evident given that a 48-fold loss in potency was observed upon substituting the carboxylate group with a hydrogen atom (**2** versus **3**). This loss could not be attributed to the elimination of an ionic or hydrogen-bonding interaction with the polymerase, since esterification of the carboxylic acid to a methyl ester or replacement of the carboxylic acid with a methyl group in a related series resulted in equipotent compounds.[8,11] We therefore considered that the carboxylic acid contributed to a favorable rigidification of the indole and linker segment (C16 and C17). The relative flexibility of both compounds in the free state was thus monitored by NMR spectroscopic and molecular modeling methods. First, middle-range ^{1}H coupling constants were observed for **3** ($J_{NH,H16} = 5.6$, 5.6 Hz, $J_{H16,H17} = 7.1$, 7.1 Hz) which are indicative of an average of populated torsion angles, whereas more extreme values were observed for compound **2** ($J_{NH,H16} = 7.2$ Hz, $J_{H16,H17} =$ 10.1, 4.5 Hz) which is consistent with a more defined conformation. Moreover, the ^{13}C T_1 values for the right-side segment of compound **2** were significantly shorter, thus suggesting a lower degree of flexibility relative to those of **3** (for example, 0.28 versus 0.82 for C16, 0.24 versus 0.38 for C17, and 0.59 versus 0.68 for C23; see the Supporting Information). Furthermore, our free-state molecular dynamics (MD) calculations determined that a boundlike torsion angle of approximately 50° along C16–C17 (S_2 as defined in Figure 3c) was preferentially populated for **2** (Figure 3d), whereas an additional torsion angle of −50° was also populated in **3** (Figure 3e). In summary, the presence of the acid at C16 rendered compound **2** less flexible than **3** which translates into a lower entropic cost for binding.

We previously reported a stepwise SAR that illustrated the importance of the indole and acetic acid groups to the affinity of compound **2** for the polymerase.[8] Line-broadening was observed for the resonances of H20–H22 (Figure 1e), which indicates the indole partially contacts the polymerase pocket. We also identified important differences between the free and bound states of the indole ring. The H6 of the benzimidazole is distal from the acetic acid H23 in the bound state based on the absence of the corresponding transferred NOESY peaks, whereas a ROESY crosspeak was observed between these hydrogen atoms in the free state (see the Supporting Information). We further probed this difference

using the transferred ^{13}C T_1 experiment, which was developed particularly for the purpose of identifying ligand substituents that are flexible in the free state and which become rigidified in the bound state.[9] ^{13}C T_1 data were acquired for free compound **2** and were then compared to data acquired on the same sample after adding polymerase. The percentage difference for each carbon atom is shown in Figure 3c within square brackets. High percentage changes were observed for C18, C21, and C22 (namely, they were rigidified upon binding) and a low percentage change was observed for C20 (minimal flexibility changes upon binding). One would expect this pattern upon rigidifying a flexible C17–indole torsion angle in the free state to a single bound conformation, when it is considered that the C20 C-H vector experienced only minor percentage changes because it lies along the pivotal C17–indole axis.

In conclusion, we have described a concerted approach involving SAR and structure- and dynamics-based methods for elucidating important features of the binding mode of novel benzimidazole inhibitors of HCV polymerase. We have demonstrated the utility of these ligand-focused methods when applied early in the drug-discovery process, such as the validation of HTS hits for lead identification, thus providing an additional NMR screening strategy that can compliment STD[10] and SAR by NMR spectroscopic methods.[10] We have also demonstrated its utility as a medicinal chemistry tool for optimization of compound potency. In the examples described here, and in the design of HCV protease inhibitors reported elsewhere,[5,11] they have been particularly valuable in the absence of X-ray structural information of a complex, a dilemma frequently encountered at the early stages of drug discovery. Despite this situation, the information described here has further potential value for medicinal chemistry purposes, and several avenues are currently under evaluation.[12] For example, rigidified analogues could be designed that mimic the bioactive conformation and reduce entropic costs upon binding. Given that large percentage transferred ^{13}C T_1 values were observed for the indole and furan rings (Figure 3c, numbers within square brackets), analogues that rigidify the C17–indole and C2–furan torsion angles should improve potency. Also, a diversity of functional groups could replace the acid at C16 as long as the indole and linker segments are adequately rigidified. Finally, the 3D bound structures and DLB data of **2** may be useful in determining the first model of a complex using an apo crystal structure of HCV polymerase, as we have done successfully in our HCV protease inhibitor program.[5] This approach could be guided by the recently proposed polymerase binding site near Pro 495 for a related benzimidazole–cyclohexyl compound that was determined by cell culture resistance studies.[13] Notably, these resistance studies suggest that the benzimidazole inhibitors bind distal to the active-site tunnel and at a distinct site from other classes of inhibitors reported to date,[14] and thus further highlights the potential "drugability" of HCV polymerase.

Received: April 14, 2004 [Z460326]

Keywords: drug design · hepatitis C virus · molecular modeling · NMR spectroscopy · structure–activity relationships

[1] a) Q.-L. Choo, G. Kuo, A. J. Weiner, L. R. Overby, D. W. Bradley, M. Houghton, *Science* **1989**, *244*, 359; b) G. Kuo, Q.-L. Choo, H. J. Alter, G. L. Gitnick, A. G. Redeker, R. H. Purcell, T. Miyamura, J. L. Dienstag, M. J. Alter, C. E. Stevens, *Science* **1989**, *244*, 362; c) A. M. Di Bisceglie, *Lancet* **1998**, *351*, 351. d) World Health Organization, *J. Virol. Hepatol.* **1999**, *6*, 35.

[2] a) G. Chander, M. S. Sulkowski, M. W. Jenckes, M. S. Torbenson, H. F. Herlong, E. B. Bass, K. A. Gebo, H *epatology* **2002**, *36*, S135; b) S.-L. Tan, A. Pause, Y. Shi, N. Sonenberg, *Nat. Rev. Drug Discovery* **2002**, *1*, 867; c) A. M. Di Bisceglie, J. McHutchison, C. M. Rice, *Hepatology* **2002**, *35*, 224.

[3] a) S. E. Behrens, L. Tomei, R. De Francesco, *EMBO J.* **1996**, *15*, 12; b) A. A. Kolykhalov, K. Mihalik, S. M. Feinstone, C. M. Rice, *J. Virol.* **2000**, *74*, 2046; c) K. E. Reed, C. M. Rice, *Curr. Top. Microbiol. Immunol.* **2000**, *242*, 55.

[4] G. McKercher, P. Beaulieu, D. Lamarre, S. LaPlante, S. LeFebvre, C. Pellerin, L. Thauvette, G. Kukolj, *Nucleic Acids Res.* **2004**, *32*, 422.

[5] a) S. R. LaPlante, D. R. Cameron, N. Aubry, S. Lefebvre, G. Kukolj, R. Maurice, D. Thibeault, D. Lamarre, M. Llinàs-Brunet, *J. Biol. Chem.* **1999**, *274*, 18618; b) S. R. LaPlante, N. Aubry, P. Bonneau, G. Kukolj, D. Lamarre, S. Lefebvre, H. Li, M. Llinàs-Brunet, C. Plouffe, D. R. Cameron, *Bioorg. Med. Chem. Lett.* **2000**, *10*, 2271; c) Y. Tsantrizos, G. Bolger, P. Bonneau, D. R. Cameron, N. Goudreau, G. Kukolj, S. R. LaPlante, M. Llinàs-Brunet, H. Nar, D. Lamarre, *Angew. Chem.* **2003**, *115*, 1394; *Angew. Chem. Int. Ed.* **2003**, *42*, 1356.

[6] F. Ni, *Prog. Nucl. Magn. Reson. Spectrosc.* **1994**, *26*, 517.

[7] P. L. Beaulieu, M. Bös, Y. Bousquet, G. Fazal, J. Gauthier, J. Gillard, S. Goulet, S. LaPlante, M.-A. Poupart, S. Lefebvre, G. McKercher, C. Pellerin, V. Austel, G. Kukolj, *Bioorg. Med. Chem. Lett.* **2004**, *14*, 119.

[8] P. L. Beaulieu, M. Bös, Y. Bousquet, P. DeRoy, G. Fazal, J. Gauthier, J. Gillard, S. Goulet, M.-A. Poupart, S. Valois, G. McKercher, G. Kukolj, *Bioorg. Med. Chem. Lett.* **2004**, *14*, 967.

[9] S. R. LaPlante, N. Aubry, R. Deziel, F. Ni, P. Xu, *J. Am. Chem. Soc.* **2000**, *122*, 12530.

[10] a) B. Meyer, T. Peters, *Angew. Chem.* **2003**, *115*, 890; *Angew. Chem. Int. Ed.* **2003**, *42*, 864; b) S. B. Shuker, P. J. Hajduk, R. P. Meadows, S. W. Fesik, *Science* **1996**, *274*, 1531.

[11] D. Lamarre, P. C. Anderson, M. Bailey, P. Beaulieu, G. Bolger, P. Bonneau, M. Bös, D. R. Cameron, M. Cartier, M. G. Cordingley, A.-M. Faucher, N. Goudreau, S. H. Kawai, G. Kukolj, L. Lagacé, S. R. LaPlante, H. Narjes, M.-A. Poupart, J. Rancourt, R. E. Sentjens, R. St George, B. Simoneau, G. Stelnmann, D. Thibeault, Y. S. Tsantrizos, S. M. Weldon, C.-L. Yong, M. Llinàs-Brunet, *Nature* **2003**, *426*, 186.

[12] P. Beaulieu, M.-A. Poupart, unpublished results.

[13] L. Tomei, S. Altamura, L. Bartholomew, A. Biroccio, A. Cessacci, L. Pacini, F. Narjes, N. Gennari, M. Bisbocci. I. Incitti, L. Orsatti, S. Harper, I. Stansfield, M. Rowley, R. De Francesco, G. Migliaccio, *J. Virology* **2002**, *77*, 13225.

[14] a) D. Dhanak, K. J. Duffy, V. K. Johnston, J. Lin-Goerke, M. Darcy, A. N. Shaw, B. Gu, C. Silverman, A. T. Gates, M. R. Nonnemacher, D. L. Earnshaw, D. J. Casper, A. Kaura, A. Baker, C. Greenwood, L. L. Gutshall, D. Maley, A. DelVecchio, R. Macarron, G. A. Hofmann, A. Alnoah, H.-Y. Cheng, G. Chan, S. Khandekar, R. M. Keenan, R. T. Sarisky, *J. Biol. Chem.* **2002**, *277*, 38322; b) L. Chan, T. J. Reddy, M. Proulx, S. K. Das, O. Pereira, W. Wang, A. Siddiqui, C. G. Yannopoulos, C. Poisson, N. Turcotte, A. Drouin, M. H. Alaoui-Ismaili, R. Bethell, M. Hamel, L. L'Heureux, D. Bilimoria, N. Nguyen-Ba, *J. Med. Chem.* **2003**, *46*, 1283; c) M. Wang, K. K.-S. Ng, M. M. Cherney, M. Maia, L. Chan, C. G. Yannopoulos, J. Bedard, N. Morin, N. Nguyen-Ba, M. H. Alaoui-Ismaili, R. C. Bethell, M. N. G. James, *J. Biol. Chem.* **2003**, *278*, 9489.

